Multi-band polarization insensitive metamaterial absorber with dual cross-wires structure*

YAO Li-fang (姚丽芳), **LI Min-hua** (李敏华), **ZHAI Xiao-min** (翟孝敏), **WANG Hui-bo** (汪会波), **and DONG Jian-feng** (董建峰)**

College of Information Science and Engineering, Ningbo University, Ningbo 315211, China

(Received 14 August 2015)

A five-band metamaterial absorber (MMA) based on a simple planar structure is proposed. It utilizes different areas of a single unit cell to match impedance, and produces different absorptive frequencies. Numerical calculation shows that the MMA has five different absorption peaks at 3.78 GHz, 7.66 GHz, 10.9 GHz, 14.5 GHz and 16.7 GHz, and their absorption rates reach 95.5%, 98.6%, 95.7%, 96.6% and 99.8%, respectively. The proposed structure is polarization insensitive for transverse electric (TE) and transverse magnetic (TM) incident waves. Also, the absorptive characteristics over large incident angles are examined. In addition, we analyze the absorption mechanism by the surface current density and power flow density distributions. This simple structure provides a way to design multi-band MMA, and also saves the cost of fabrication.

Document code: A **Article ID:** 1673-1905(2015)06-0414-4

DOI 10.1007/s11801-015-5157-0

Since the first metamaterial absorber (MMA) was presented by Landy[1] achieving narrow band absorption at microwave frequency, the metamaterial applied to perfect absorption has attracted great attention. The MMA generally consists of three layers: two metallic layers separated by a dielectric layer. Because of the perfect combination, MMA breaks the traditional absorber of the resistive sheet with $\lambda_0/4$, where λ_0 is the wavelength in free space. Also, polarization dependence[2,3] and polarization independence[4,5], large incident angle[6,7], multi-band[8,9] and broadband[10,11], tunable MMAs[12,13] are achieved. But there are still some issues focused on MMA, for example, its working bandwidth is relatively narrow, and its absorptive frequency can't be adjusted flexibly. To overcome the narrow band limit, many researchers have taken attention to achieve the multi-band and broadband absorption. There are different methods to achieve it, for example, a multi-band absorber by using the same shape cells with different sizes[14], an ultra-broadband absorber utilizing the alternating layers of flat metal and dielectric plates[15], a broadband MMA based on lumped elements[16], the absorber consisting of a metallic planar spiral layer to produce triple bands[17] and a new approach by using a genetic algorithm to overcome the dual-band problem[18].

In this paper, we utilize a single unit cell to match impedance at different positions for different resonance frequencies. This method has been used to produce multiple bands in the past, but their structures of MMAs are often complex[19]. Now we use a simple structure and achieve perfect absorption at five resonance frequencies. The proposed MMA is polarization insensitive and can remain five absorption peaks with high absorption over large incident angles. Also, the effect of parameters on absorption is analyzed. In addition, we examine the absorption mechanism by the surface current density and the power flow density distributions.

As described in Fig.1, the unit cell of the MMA includes three layers. The front layer is made of two crossed metal trips, the back layer is a thick metal layer, and the two layers are separated by a dielectric layer. Metal layers are made of copper, and its conductivity is 5.8×10^7 S/m. FR-4 is selected as substrate, and its dielectric constant and dielectric loss tangent are 4.3 and 0.025, respectively. The simulated MMA has the dimensions of a=20 mm, b=17.5 mm, c=2 mm, w=0.6 mm and t=1.9 mm. The thickness of metal layers is 0.017 mm.

Finite integration technique is used to perform the simulation. The unit cell is set according to the periodic boundary conditions in the x-y plane, and opens along the z-direction for the propagation. The transmission

* This work has been supported by the National Natural Science Foundation of China (No.61475079), the Ningbo Optoelectronic Materials and Devices Creative Team (No.2009B21007), the Educational Committee of Zhejiang Province (No.Y201430863), the Ningbo Natural Science Foundation (No.2014A610144), the Scientific Research Foundation of Graduate School of Ningbo University (No.G15056), and the K. C. Wong Magna Fund in Ningbo University.

** E-mail: dongjianfeng@nbu.edu.cn

coefficient $|S_{12}|$ can be considered as zero, as the back metal layer blocks the incident wave. So the absorption can be calculated as $A=1-|S_{11}|^2$, where $|S_{11}|$ is the reflection coefficient.

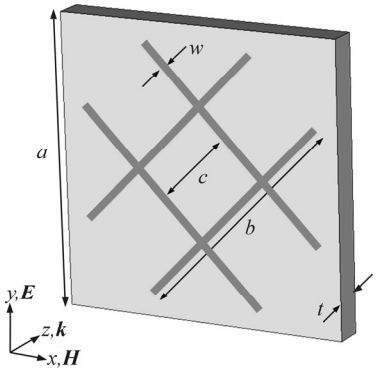

Fig.1 Schematic diagram of the unit cell with dual cross parallel wires structure

The absorption spectrum of the MMA based on the simple structure is shown in Fig.2. It can be seen that five absorption peaks have the uniform absorption at f_1=3.78 GHz, f_2=7.66 GHz, f_3=10.9 GHz, f_4=14.5 GHz and f_5=16.7 GHz with the absorption rates of 95.5%, 98.6%, 95.7%, 96.6% and 99.8%, respectively. Higher absorption rates can be obtained by choosing the dielectric with higher dielectric losses.

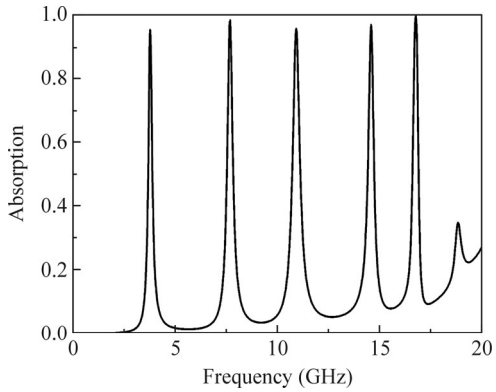

Fig.2 Absorption spectrum of the MMA

To confirm the polarization insensitivity of the absorber, we simulate the absorption spectra at different polarization angles. In Fig.3, we can see that the absorption peaks overlap at the polarization angles from 0° to 45° by the step of 15°, which means that the absorber can work well at different polarization angles.

To test the absorption performance at large incident angles, we simulate the absorption spectra at different incident angles. Fig.4 shows that the absorption spectra remain five peaks, and the peak wavelengths do not change when the incident angles are 0° and 15°. While the incident angle is 30°, for transverse electric (TE) polarization, the former three peaks keep the same, but the absorption rates seem to be reduced to some degree. This is because the direction of the magnetic field of incident waves is changed, so that the magnetic field cannot drive the circulating currents at some frequencies[20]. For transverse magnetic (TM) polarization, the first three absorption rates remain unchanged. It can be explained that the magnetic field drives the circulating currents effectively at large incident angles. In addition, several frequencies drift in the high frequency range for TE and TM waves when the incident angle is 30°. It is because the current distributions of adjacent unit cells are different when the incident angle is increased at the high frequency.

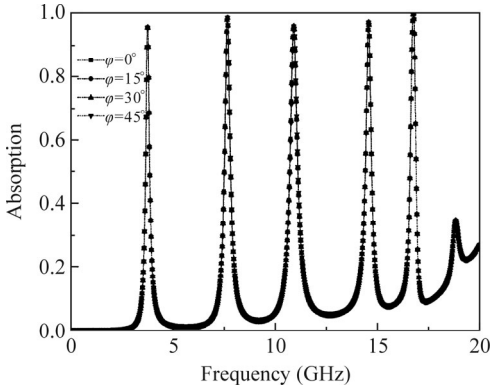

Fig.3 Absorption spectra of MMA at different polarization angles

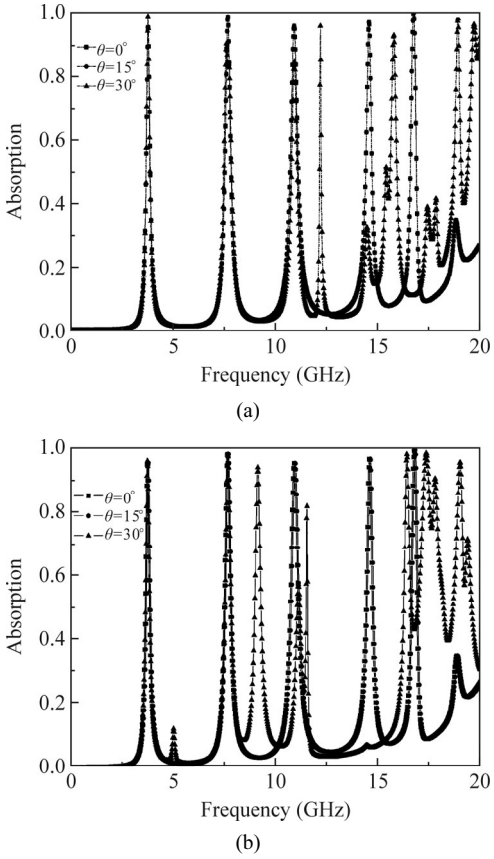

Fig.4 Absorption spectra of MMA at different incident angles for (a) TE mode and (b) TM mode

To adjust the absorptive frequencies more easily, we also study the effects of parameters on absorption spectrum. Fig.5 describes the absorption spectra of MMA with different thicknesses of *t*. From Fig.5, we can find that the fourth and the fifth absorption peaks are shifted to the lower frequency, and the absorption is reduced slightly when the thickness is increased from 1.7 mm to 2.1 mm. But the thickness *t* has litte effect on other frequencies. Also, we discuss the effect of the distance *c* between two strips on the absorption. From Fig.6, we can find that the seconed absorption peak is blue shifted, while the third absorption peak is red shifted when *c* is increased from 2.4 mm to 2.8 mm. Meanwhile, the absorption remains nearly uniform, and the parameters do not affect other frequecies. From the discussion above, we can see that the different absorption frequencies are sensitive to the different paramaters of the strucutrue. We can adjust the interesting absorption frequency by changing the parameter. At the same time, the absoption is nearly unchanged and can remain high absorption by changing the parameter.

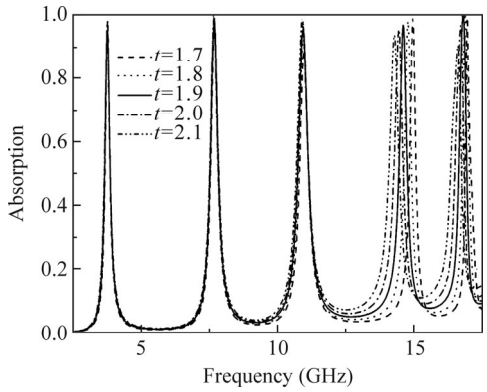

Fig.5 Absorption spectra of MMA with the thickness of *t* changed from 1.7 mm to 2.1 mm

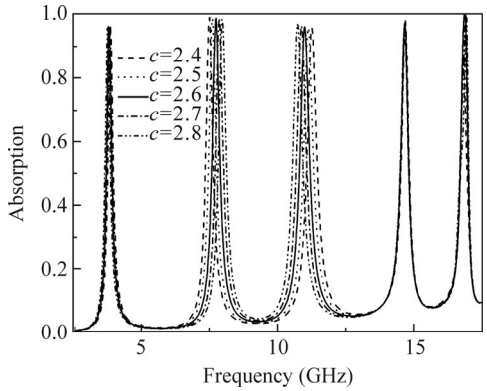

Fig.6 Absorption spectra of MMA with the distance between two strips of *c* changed from 2.4 mm to 2.8 mm

In order to understand the physical mechanism of MMA, the field distribution analysis is described. Fig.7 shows the surface current density distributions at the front layer and the back layer and the power flow density distributions with the absorptive frequencies at f_1=3.78 GHz, f_2=7.66 GHz, f_3=10.9 GHz, f_4=14.5 GHz and f_5=16.7 GHz, respectively. The arrow indicates the direction of flow. At f_1, f_2 and f_3, the current directions at front and back layers are antiparallel, and current loop is driven by the *H*-field, leading to the magnetic resonance. Meanwhile, the current directions at front and back layers are parallel at f_4 and f_5, which means that the current density distribution no longer contributes to the magnetic resonance. At all the resonant peaks, the oscillating currents are driven by the *E*-field in front and back layers, yielding the electric resonance through metal trips and metal sheets.

In addition, different portions of the unit cell separately couple to the incident electromagnetic wave, leading to perfect absorption at different resonance frequencies. We can see that the power flow is mostly localized in the middle of the rods in Fig.7(a), the power flow is mostly localized in the partial arms of the structure in Fig.7(b), the power flow is mostly localized in the cross points of the rods and the arms of the structure in Fig.7(c), the power flow is mostly localized in all cross points of the rods in Fig.7(d), and the power flow is mostly localized in partial cross points of the rods in Fig.7(e). But the absorption of MMA is mainly from the dielectric loss as the simulated result shown in Fig.8. The absorption spectra with the lossy dielectric and the lossless dielectric are shown in Fig.8. Consequently, the electromagnetic energy is significantly reinforced in the MMA, then converted into thermal energy and consumed, leading to a perfect absorption.

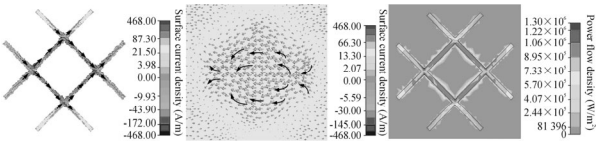

(a) 3.78 GHz

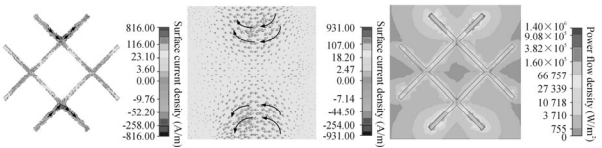

(b) 7.66 GHz

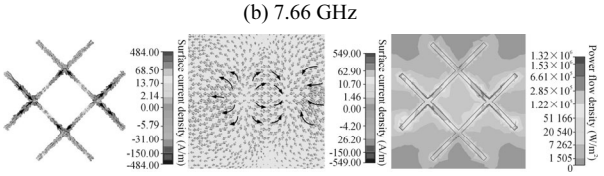

(c) 10.9 GHz

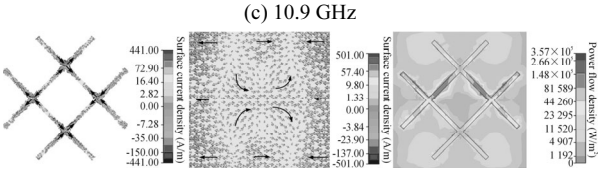

(d) 14.5 GHz

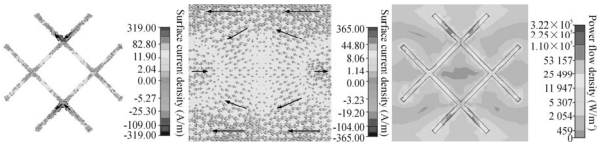

(e) 16.7 GHz

Fig.7 The surface current density distributions at the front layer (left row) and back layer (middle row), and the power flow density distributions (right row) of the MMA at five different resonant frequencies

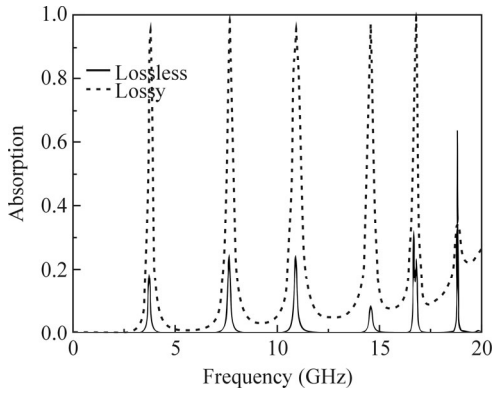

Fig.8 Absorption spectra of MMA with lossless and lossy dielectrics

In summary, we present a five-band polarization insensitive MMA using a simple structure. Numerical calculation results indicate that the absorption rates exceed 95% at the five different absorptive peaks in the vertical incidence, and we can adjust the resonance frequency by changing the parameter of the structure. Also, the MMA is polarization insensitive and can achieve several resonance frequencies with high absorption at large incident angles for TE and TM incidence waves. The physical mechanism of absorption is studied, which shows that perfect absorption of five-band is achieved by matching the impedance at the five different positions of the unit cell. The proposed MMA can be used as spectrally sensitive detectors and sensors, and can save the cost of the fabrication. Also, it can be integrated to electronic equipment to avoid electromagnetic compatibility.

References

[1] N. Landy, S. Sajuyigbe, J. Mock, D. Smith and W. Padilla, Physical Review Letters **100**, 20 (2008).

[2] C. Hu, X. Li, Q. Feng, X. N. Chen and X. Luo, Optics Express **18**, 7 (2010).

[3] Q. Y. Wen, H. W. Zhang, Y. S. Xie, Q. H. Yang and Y. L. Liu, Applied Physics Letters **95**, 24 (2009).

[4] S. O'brien, D. McPeake, S. Ramakrishna and J. Pendry, Physical Review B **69**, 24 (2004).

[5] N. I. Landy, C. M. Bingham, T. Tyler, N. Jokerst, D. R. Smith and W. J. Padilla, Physical Review B- Condensed Matter and Materials Physics **79**, 12 (2009).

[6] B. Zhu, Z. B. Wang, Z. Z. Yu, Q. Zhang, J. M. Zhao, Y. J. Feng and T. Jiang, Chinese Physics Letters **26**, 11 (2009).

[7] L. Huang, D. R. Chowdhury, S. Ramani, M. T. Reiten, S. N. Luo, A. K. Azad, A. J. Taylor and H. T. Chen, Applied Physics Letters **101**, 10 (2012).

[8] H. Tao, C. Bingham, D. Pilon, K. Fan, A. Strikwerda, D. Shrekenhamer, W. Padilla, X. Zhang and R. Averitt, Journal of Physics D: Applied Physics **43**, 22 (2010).

[9] X. Shen, T. J. Cui, J. Zhao, H. F. Ma, W. X. Jiang and H. Li, Optics Express **19**, 10 (2011).

[10] Q. Liang, T. Wang, Z. Lu, Q. Sun, Y. Fu and W. Yu, Advanced Optical Materials **1**, 1 (2013).

[11] S. Li, J. Gao, X. Cao, W. Li, Z. Zhang and D. Zhang, Journal of Applied Physics **116**, 4 (2014).

[12] W. Zheng, W. Li and S. J. Chang, Optoelectronics Letters **11**, 18 (2015).

[13] C. H. Wang, D. F. Kuang, S. J. Chang and L. Lin, Optoelectronics Letters **9**, 266 (2013).

[14] J. W. Park, P. V. Tuong, J. Y. Rhee, K. W. Kim, W. H. Jang, E. H. Choi, L. Y. Chen and Y. P. Lee, Optics Express **21**, 8 (2013).

[15] Y. Cui, K. H. Fung, J. Xu, H. Ma, Y. Jin, S. He and N. X. Fang, Nano Letters **12**, 3 (2012).

[16] Y. Z. Cheng, Y. Wang, Y. Nie, R. Z. Gong, X. Xiong and X. Wang, Journal of Applied Physics **111**, 4 (2012).

[17] X. Huang, H. Yang, S. Yu, J. Wang, M. Li and Q. Ye, Journal of Applied Physics **113**, 21 (2013).

[18] Z. H. Jiang, S. Yun, F. Toor, D. H. Werner and T. S. Mayer, ACS Nano **5**, 6 (2011).

[19] H. X. Xu, G. M. Wang, M. Q. Qi, J. G. Liang, J. Q. Gong and Z. M. Xu, Physical Review B- Condensed Matter and Materials Physics **86**, 20 (2012).

[20] N. Liu, M. Mesch, T. Weiss, M. Hentschel and H. Giessen, Nano Letters **10**, 7 (2010).